Chapter 4:

SEISMOTECTONICS OF NW HIMALAYA

Chapter 4:

Seismotectonics of the Western Himalayan segment, NW Himalaya, India

4.1.Introduction

In the previous chapter, the initial 1D crustal velocity model was obtained using the P and S wave travel time inversion. Since, the region falls under an active seismicity and tectonic processes, hence, in this chapter the study is focussed mainly on the Microseismic activity, tectonic and the estimation of the slip potential for the NW Himalayan region, India. As it is well known that that any tectonically disturbed region that has produced Great earthquakes ($M \geq 8.0$) can also produce the same in future. Therefore there is an immense necessity for the Microseismic study of these areas using different advanced seismological techniques. The present study aims at delivering some of the interesting and new insights into the Active tectonics of the area. The research objectives are achieved by using a newly estimated 1D local crustal velocity model for earthquake relocations in the study area. The spatial-temporal seismicity pattern have been studied by utilizing the HYPODD program (Wald Hauser and Ellsworth, 2000) incorporating the calculated 1D local crustal velocity model for the area. The source characteristics of the area is also studied by the determinations of the focal mechanisms or Moment tensors using waveform inversion of local and regional waveforms having a magnitude ($Mw \geq 4$) for the study region. This study is carried out by utilizing the grid search method of waveform inversion technique (Sokos and Zahradnik, 2007). Hence, the present study provides more precise earthquake locations with reduced errors in the estimated location parameters (Latitude, Longitude and Depth) as compared to the previous studies attempted by various researchers. The P and S phase are used to determine the relative arrival time pairs. The earthquake potential prevailing in the region has also

estimated taking into consideration the amount of energy accommodated and the amount of energy released through past events. Fault-plane solutions derived from seismicity in the Himalaya-Tibet region which characterise the first-order deformation patterns. The moment tensors reported south of Tibetan Plateau, documented pure normal faulting, indicating E–W extension, both at shallow crustal levels (<15 km) and at greater depths of 80–95 km (Molnar and Chen, 1983; Molnar and Lyon-Caen, 1989). In contrast, earthquakes in the Himalaya with magnitudes of up to 8.0 are reported to have a thrusting focal mechanisms and are located at depths between 20 and 40 km and these earthquakes are primarily related to the underthrusting of India beneath Eurasia (e.g., Seeber and Armbuster,1981; Ni and Barazangi, 1984). The precise and improved earthquake locations, energy stored for future giant event along with the estimated Fault plane solutions allowed us to constrain the geometry of the active faults, predict the magnitude of the future seismic event and decode the seismotectonics in the NW Himalaya region. *Figure 4.1* shows general seismotectonic map of the NW Himalaya showing the epicentre of 1905 Kangra earthquake and 1975 Kinnaur earthquake. Major tectonic breaks along with the NE-SW transect AB.

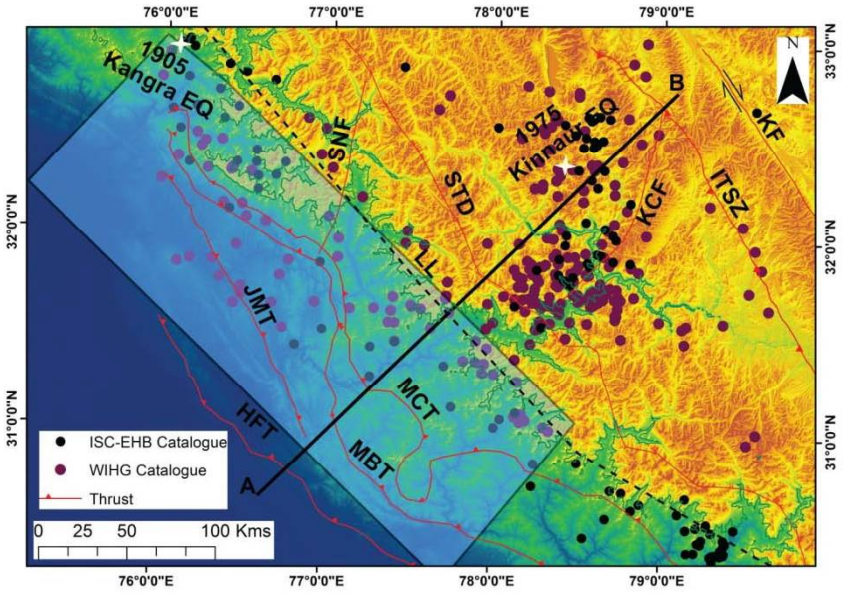

Figure 4.1: General Seismotectonic map of the NW Himalaya showing the epicentre of 1905 Kangra earthquake and 1975 Kinnaur earthquake. Major

tectonic breaks ITSZ: Indus-Tsangpo Suture Zone; MCT: Main Central Thrust; MBT: Main Boundary Thrust; HFT: Himalayan Frontal Thrust; JMT: Jawalamukhi Thrust; KCF: Kaurik-chango Fault; SNF: Sundarnager Fault along with the topography as well as the focal mechanism solutions of some major earthquakes that occurred in the region in the past (Modified from GSI, 1993). The map also shows the relocated earthquake epicentres. LL: The dotted line is designated as locking line (Bollinger et al., 2004). The shadow rectangle signifies the western Himalaya seismic gap between the epicentre of 1905 Kangra earthquake (Mw = 7.8) and 1975 Kinnaur earthquake (Mw = 6.8). The NE-SW transect AB is also shown in the figure.

Station Name	**Station code**	**Latitude (°N)**	**Longitude (°E)**	**Elevation (m)**
SARHAN	SRHN	31.533	77.792	1983
RACKCHHAM	RKCH	31.393	78.356	3129
SPILO	SPLO	31.650	78.441	2353
KHAB	KHAB	31.469	78.644	2715
HURLING	HURL	32.062	78.551	3190
MUDH	MUDH	31.963	78.038	3811
KAZA	KAZA	32.219	78.072	3701
LOSSER	LOSR	32.435	77.750	4141
PULGA	PULG	31.995	77.452	2274
BANZAR	BNJR	31.645	77.348	1369
DEOL	DEO	32.093	76.672	700
CHHATRARI	CHT	32.440	76.372	1800
LAGORE	LGR	32.292	75.907	800
UNA	UNA	31.520	76.318	550

Table 4.1: Seismic stations details operated by Wadia Institute of Himalayan Geology (WIHG) in the NW Himalaya.

4.2. Initial earthquake locations with Hypo71

The recorded earthquake waveforms are analysed for earthquake hypocenter locations using the SEISAN software (Havskov and Ottemueller, 1999), which utilizes the HYPO71 program (Lee and Lahr, 1975) for earthquake locations. *Table 4.1* summarizes the station information used in the network. These estimated parameters with the initial 1 D velocity model of Kumar et al., 2009 is seen to have much more error associated with the hypocentral parameters. As mentioned in the earlier Chapter 3 that the root mean square (rms) obtained with the hypocenter locations with this initial velocity model is 0.87s. This leads to spare distribution of hypocenters in the area. The seismic stations used for estimating initial epicenter locations are shown in *Table 4.1.*

After estimating the preliminary hypocentral parameters using a predefined five layered velocity model derived by Kumar et al., 2009, the earthquake hypocenters are recalculated using the newly calculated 1 D crustal velocity model as discussed is shown in *Table 4.2* with the HypoDD technique (Waldhauser and Ellsworth, 2000). The purpose of using this velocity model for preliminary earthquake location is the resultant low root mean square (rms) obtained with the hypocenter locations.

4.3. Relocating the earthquake hypocenters in the NW Himalaya utilizing HypoDD

The HypoDD technique is based on the principle that the ray paths between the different hypocentres and the recording common stations are similar if the distances between the hypocentres are small as compared to the event- station distance and the scale- length of velocity heterogeneity. (Frechet, 1985; Got, et al., 1994). Then the travel time residual for the event pairs observed at common recording stations were minimized by iteratively adjusting the vector difference between the hypocentral parameters. The differential travel times of P-wave and S-wave arrivals and initial locations determined from HYPO71 (LEE and Lahr, 1975) are used as an input for the HYPODD (Waldhauser and Ellsworth, 2000). Utilizing 4495 P and 4453 S arrival times, out of a total 466 events 423 are relocated by HypoDD using the

conjugate gradient method (LSQR). This technique utilized the earthquakes whose magnitude lies between M_L 1.0 and 6.0 for relocation in the study region. In this way a total number of 423 earthquakes having 13 or more (P and S) phases are considered for relocation. The parameterization considered for selecting the events for relocation are as follows:

1)The maximum distance between the station and the event pairs is 200 Km

2) The maximum hypocentral separation between the event pairs is 25 Km

3)The maximum number of neighbours per event is fifteen and the minimum number of events required to define a neighbour is twenty links.

4)On an average a total of thirteen P and S differential times resulted for each event pair. The average rms for the travel time residual was found to be $\leq$ 0.2 s for all the earthquakes relocated using the arrival times from at least three seismographs.

Depth (Km)	**P wave Velocity (Km/s)**	**S wave Velocity (Km/s)**
0	5.219	2.998
5	5.314	3.015
10	5.391	3.134
15	5.392	3.135
20	5.964	3.441
25	6.071	3.482
30	6.313	3.647

Table 4.2: Crustal 1 D velocity model utilized for earthquake relocations with HypoDD.

4.4. Relocated hypocenters and reduced errors in terms of hypocentral parameters

The accuracy in obtaining the absolute hypocenter locations depends upon various factors that include mainly the network geometry, available phases, arrival-time reading accuracy, and knowledge of the crustal structure

(Pavlis, 1986; Gomberg et al., 1990). When one-dimensional reference velocity model is used to locate the earthquakes, it limits the location accuracy, since three-dimensional velocity variations can introduce systematic biases into the estimated travel times. This can partially be controlled by including station and/or source terms in the location procedure (e.g., Douglas, 1967; Pujol, 1988; Hurukawa and Imoto, 1992; Shearer, 1997) and/or by jointly inverting the travel-time data for hypocenters and velocity structure (e.g., Crosson, 1976; Ellsworth, 1977; Roecker, 1981; Thurber, 1983; Michael, 1988; Kissling et al., 1994). So the double-difference technique of Waldhauser and Ellsworth, 2000 has been utilised to have a minimum residuals in the hypocentral parameters in the study region. In the present context, the earthquake hypocenters are relocated according to its spatial distribution along the latitude, longitude and depth. Unlike the epicentral distribution obtained using HYPO71, the relocated events reveal an improvement in terms of a reduced scatter and clustering in latitude, longitude and depth of the earthquake events. It can be seen from the error plots that about 90% of earthquakes are having a least error in the hypocenter parameters. The average error obtained from the error profiles for the latitude and longitude are almost equal corresponding to ≤ 200 m and for depth corresponds to ≤ 200 m for the study region. This reduction in error for the estimated hypocentral parameters is of great achievement to the spatio-temporal seismic study in the NW Himalaya region. This shows a clear picture of hypocenter distributions in the study region with a higher degree of accuracy. *Figure 4.2* shows relocated earthquake hypocenters achieved through HYPODD program are shown. The earthquake hypocenters are plotted in accordance to its respective magnitude range.*Figure 4.3* shows the reduced uncertainty in earthquake hypocentre parameters (Latitude, Longitude and Depth) achieved after the relocations.

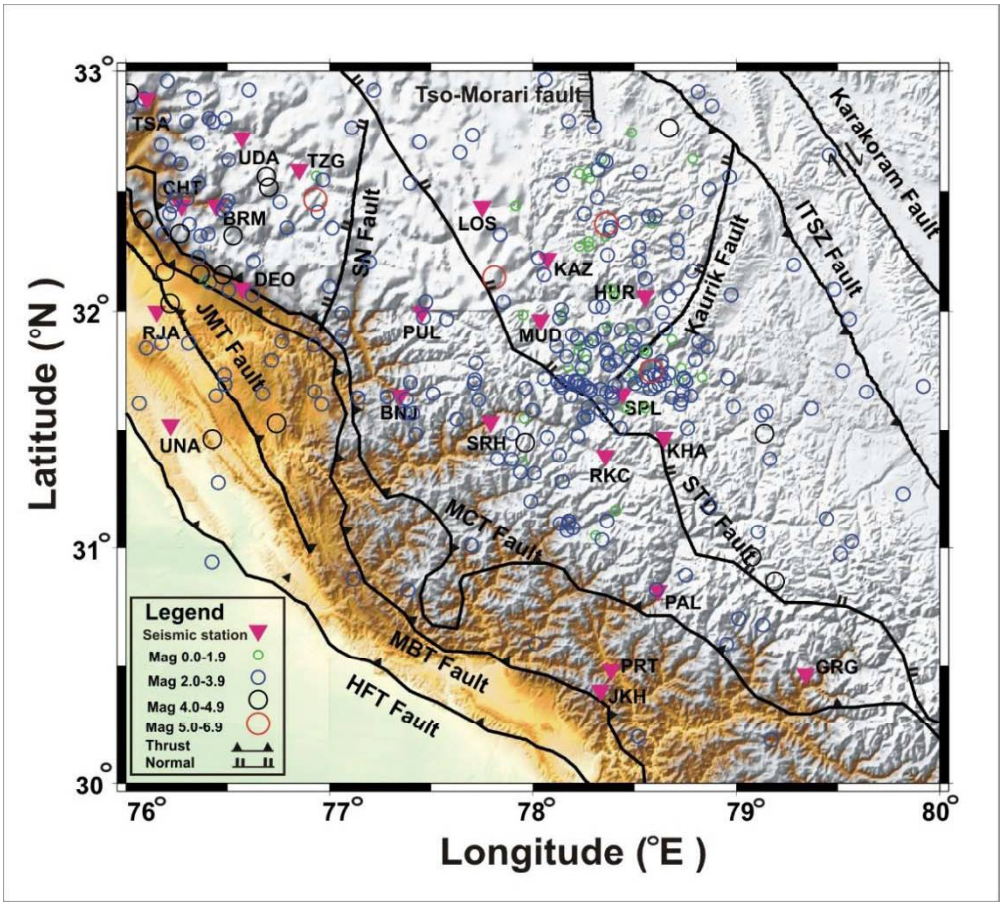

Figure 4.2: Relocated earthquake hypocenters achieved through HYPODD program are shown. The earthquake hypocenters are plotted in accordance to its respective magnitude range. Major tectonic breaks ITSZ: Indus-Tsangpo Suture Zone; STD: South Tibetan Detachment Fault; MCT: Main Central Thrust; MBT: Main Boundary Thrust; HFT: Himalayan Frontal Thrust; JMT: Jawalamukhi Thrust; KCF: Kaurik-chango Fault; SNF: Sundarnager Fault along with the topography is shown in the plot.

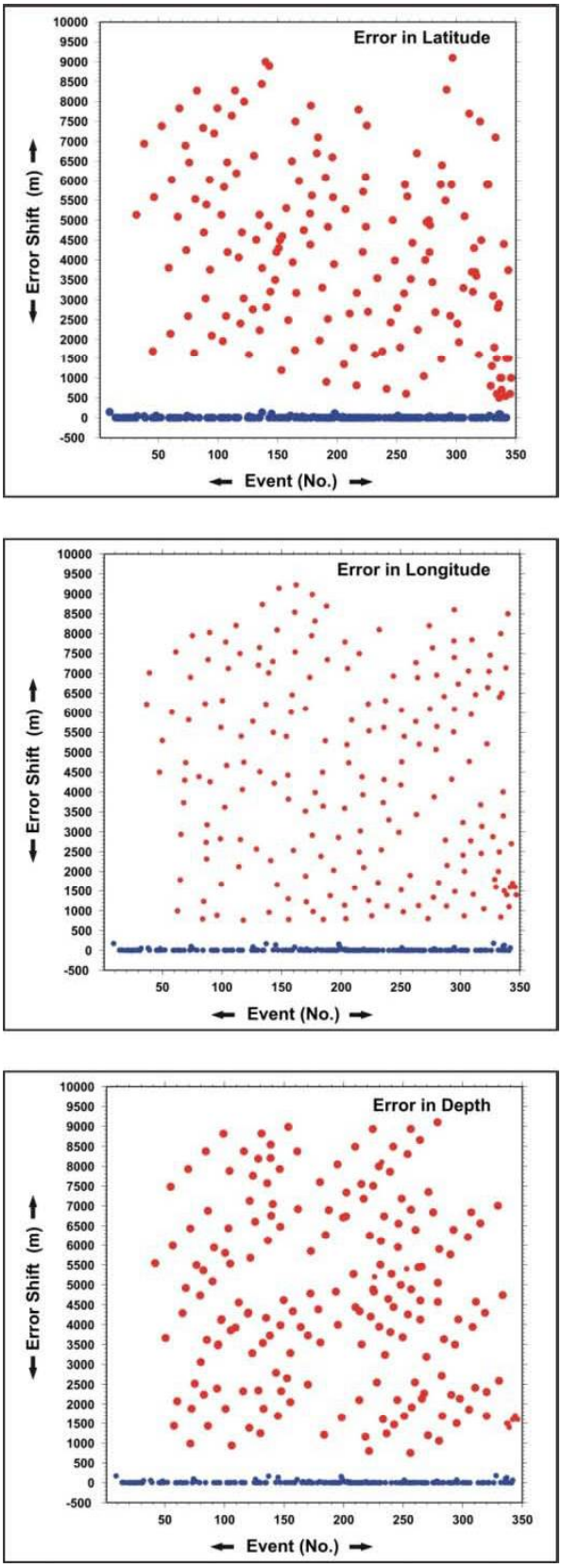

Figure 4.3: Reduced uncertainty in earthquake hypocentre parameters (Latitude, Longitude and Depth) achieved after the relocations.

4.5.Spatio-Temporal variation of seismicity from double-difference relocation

To infer the seismicity pattern in the study area, a highly precise position of the hypocenters should be estimated. This essential information's are in need for the critical analysis of the major tectonic structures in the region. The NW Himalaya is regarded as one of the most seismically active regions of the world. Earthquakes of all magnitude (small, medium, and large) have occurred in the NW Himalaya since the earliest recorded history (e.g., Gutenberg and Richter, 1954; Chandra, 1978). The seismicity distribution in the Himalayan arc does not follow a particular trend (Ni and Barzangi, 1984) though some trends are recognised in due course of time. Four great earthquakes (Ms > 8) that have occurred since 1897 in the Himalayan arc are related to the present mountain-building processes in the Himalaya (Seeber and Armbruster, 1981). Again according to the steady state model of Seeber et al., 1981, the great Himalayan earthquakes are located in a different tectonic environment than the moderate-sized Himalayan thrust events. In the present context of the study the seismicity distribution in the study region as shown in *Figure 4.1* is mainly due to the underthrusting of the Indian plate with the Eurasia plate. Earthquakes having a magnitude distribution ranging from M_L1.0 to 6.0 are considered in the study region for the hypocenter relocations. The earthquake hypocenters in the study region are mainly clustered along the major thrust faults the MBT (Main Boundary Thrust), MCT (Main Central Thrust) and the STD (South Tibetan Detachment). This seismicity distribution in this part of the Himalaya is mainly influenced by stress changes due to fault interaction between the Himalaya and Tibet, occurrence of great and major earthquakes along the arc (Gahlaut et al., 2011), and by the deviatoric stresses due to topographic variation along the arc (Bollinger et al., 2004., Mahesh et al., 2013). When the earthquakes are plotted along the N–S direction with respect to its magnitude, a clear image of highly active seismic window lying between 31.0° and 32.8 ° N were obtained. This shows a higher number of small to moderate sized earthquakes distributed in this area of approximately 200 Km with a maximum earthquakes having a range of hypocentral depth range from 5 Km to 50 Km. Again relocating earthquakes along the E–W

direction with respect to their magnitude, a clear image of highly active seismic window lying between 76.2° to 79.5 E having the same shallow focal depth distribution with maximum seismicity up to a depth of 50 Km are obtained. *Figure 4.4* shows the relocated hypocenters plotted as a function of Depth.The located and relocated earthquakes in this region show a linear pattern of seismicity distribution as compared to diffused pattern shown earlier and are mainly concentrated in a narrow active zone of lying between the MBT and MCT in the Kangra-Chamba sector and also in-between MCT and STD as well as towards the north of STD. This improved earthquake pattern provides us with valuable information on the geometry of the fault.

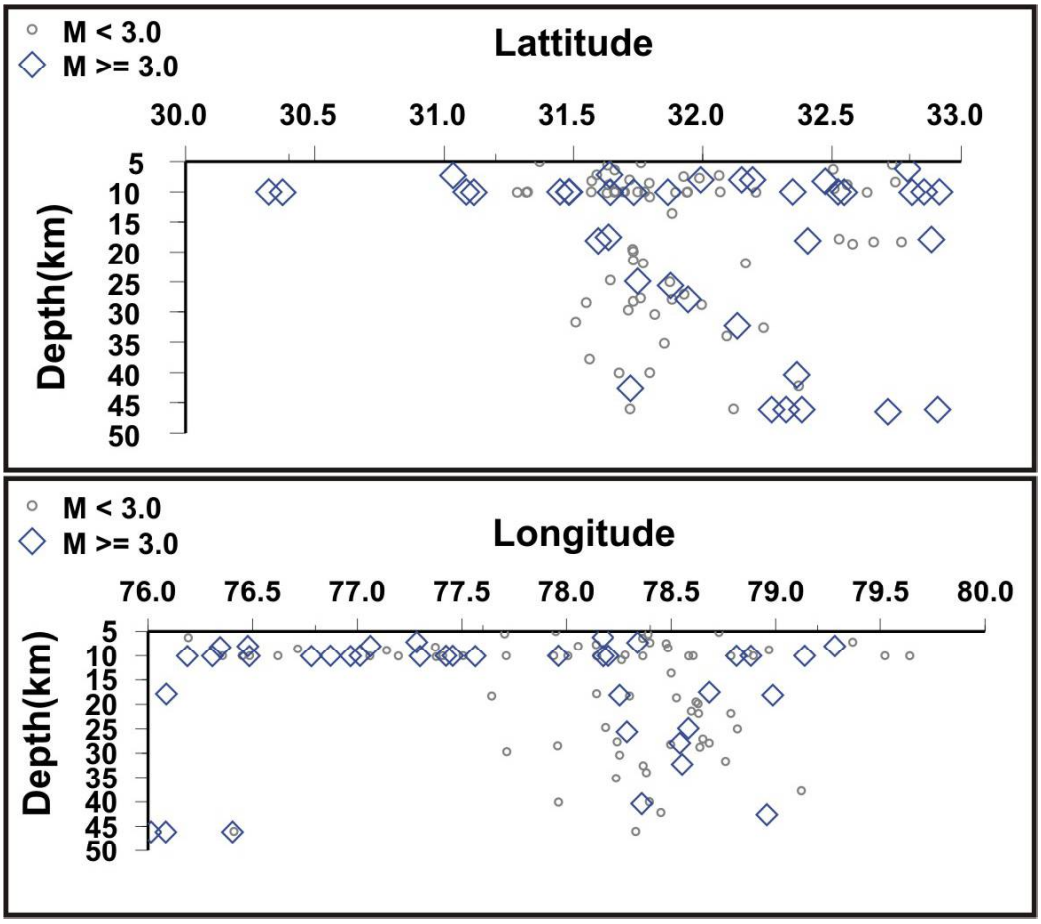

Figure 4.4: Relocated seismicity (Latitude and Longitude) plotted as a function of Depth

4.6. Moment Tensor Focal mechanisms

Earthquake relocation in the study region draws a detailed picture of the seismotectonics of the fine structure of the area, yet it does not provide more evidence about the kinematics of the tectonic regime. For this purpose, the moment tensor inversion of eight light to moderate earthquakes are performed which lies in the source region of 1905 Kangra earthquake (Ms ≥7.8) and 1975 Kinnaur earthquake (Ms ≥6.8) of the NW Himalaya. This inversion is based on the so-called iterative deconvolution of Kikuchi and Kanamori (1991), modified for regional distances and newly encoded by Zahradnik et al., 2005. The moment tensor analysis of a total of eight (8) earthquake events having a Moment magnitude (Mw) range from 4.0 to 5.0 in the NW Himalayan region is presented in the study. The MT calculation is performed using the crustal model as discussed earlier with the frequency range from 0.01–1.0 Hz. Those are the lowest frequencies with a good and satisfactory signal-to-noise ratio for such recorded seismic events (Mw≥ 4.0). The signal to noise ratio (SNR) lies between 0.05 to 1 Hz. The main reason for selecting such low frequencies for waveform modelling is because in case of low frequency, the modelling is less dependent on the inherently incomplete information of the crustal structure. The variance reduction which represents the synthetic observed waveforms fit for a moment-tensor solution is also taken into account for overall acceptance of the solution along with the DC %. The total variance reduction is considered to indicate a good fit when it is larger than 40%. There are some seismic events showing a higher amount of non-DC component and there may be several reasons to that. In the present study the crustal earthquakes with a maximum depth of 50 km in the area are considered. This is due to presence of a nearby geothermal source. The presence of such sources can be explained by opening cracks due to high pressure fluids, which is produced by a combination of shearing and opening of the fault (Panza &Saraò, 2000; Vavryčuk, 2002; Templeton and Dreger, 2006). Opening cracks might be then filled with fluids or magma. The determination and interpretation of non-DC components is particularly difficult because the non-DC components can also be generated by errors in the modelling procedure. Besides, the errors in the velocity model and an

inaccurate location of an earthquake, a sparse distribution of stations on the focal sphere and noise in data also produce so-called 'artificial' non-DC components. Furthermore, a simplified source model can generate the non-DC components. Therefore, it is important to carefully interpret the retrieved non-DC components and a detailed analysis of uncertainties of the non-DC is essential. For example, extensive synthetic tests on the sensitivity of the non-DC components for the specific setup (network geometry, distribution and characteristics of seismicity, data quality, etc.) can define a confidence level above which the retrieved non-DC components can be considered as statistically significant (Panza and Saraò, 2000). Such test reduces the misinterpretations and contributes to a profound analysis of the non-DC components.

These events are analysed with a minimum of three broad band stations to a maximum of five broadband seismic stations operated in the study area between the periods from 2010 to 2013 based on its epicentral separation and waveform quality. All of these analysed events for moment tensor determination were recorded in the miniseed format files and later converted into SAC files using the *Wavetool* program encoded in the SEISAN software package. In order to work out and pick the proper frequency band for the inversion, the signal to noise ratio at each recorded stations by utilizing the data filter tool are estimated. In the next step the *crustmod* tool are applied which converted the velocity model in to a proper ISOLA recognised format and for this the previously estimated 1 D crustal velocity model were provided for the study area.

Next steps involves input of event information, selection of stations to be used in the inversion, and raw data pre-processing, which are done using the *eventinfo, stationselect, and datain* tools. After this the trial source positions are provided using the *sourcepre* tool for single source point depth inversion provided by USGS for all the eight different earthquakes. This type of source depth inversion is quite helpful in estimating the true focal depth of the event. Then for these calculated source depths Green's function files are generated utilizing the *greenpre* tools. The inversion is carried out in frequency domain, having a frequency range of 0.05 to 0.10 Hz with cosine

tapered applied to both ends. Additionally, for tectonic interpretation the six earthquakes recorded by the USGS in the NW Himalaya are also included. These focal mechanisms are mainly dominated by thrust and normal fault plane solutions and only a few strike-slip mechanisms. In all the cases stable moment tensor estimates is obtained which reproduces well near-regional waveforms with broad azimuthal distribution. The depth estimates from moment tensor, however, show high resolution, with best estimates oscillating between 5 km and 47 km. The MT solutions of the eight seismic events determined from the present study indicate that the main types of faulting in the area are thrust having a NW–SE trend (event no. 01, 02, 03, 06 and 07) and (event no. 04, 05, and 08) Normal faulting with an N-S trend scenario.*Figure 4.5 to 4.12*shows plots of the the Real-synthetic match at various recording stations and the source depth correlation for eight different magnitudes earthquakes recorded at different seismic stations operated in NW Himalaya, India.

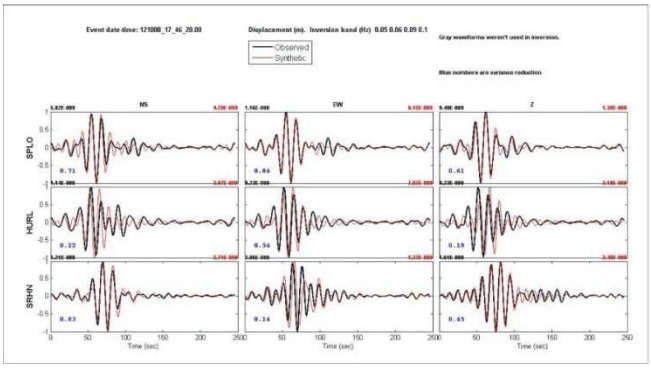

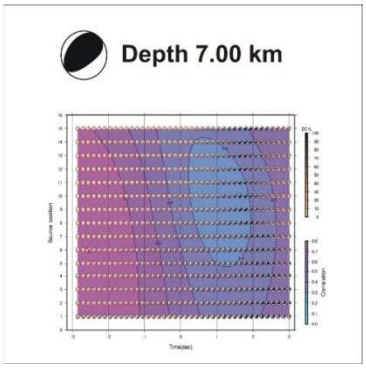

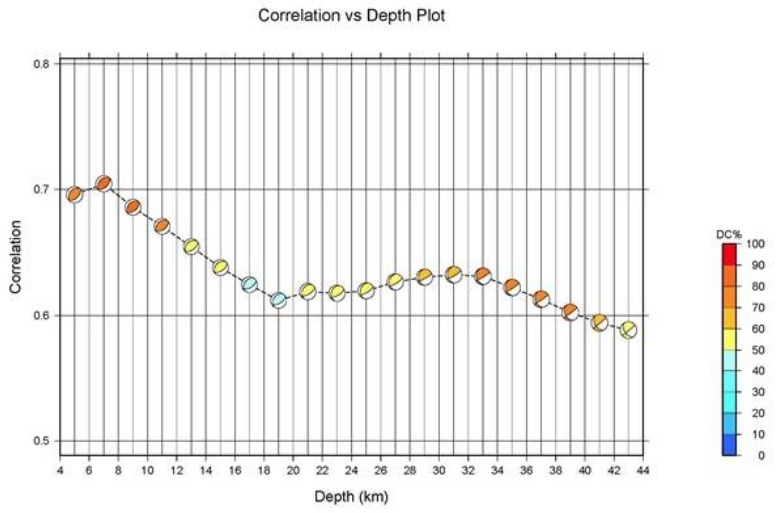

Figure 4.5: (a) and (b) showing aplot the Real-synthetic match at various recording stations and the source depth correlation for a magnitude (Mw > 5.0) earthquake recorded on date 08.10.2012.

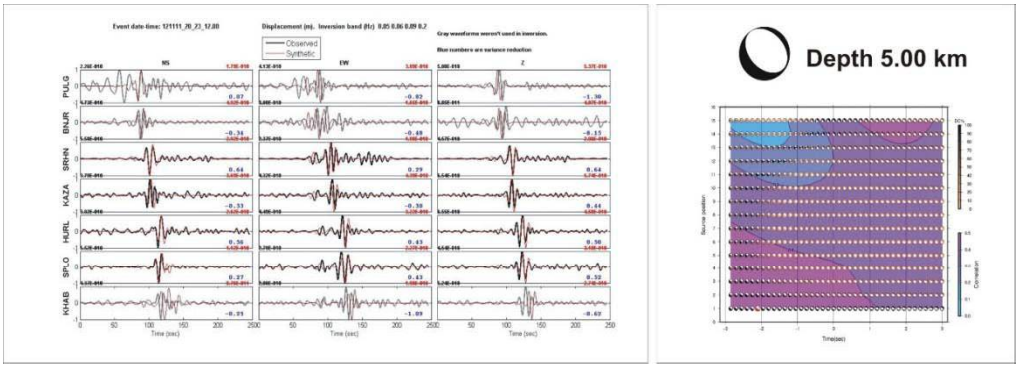

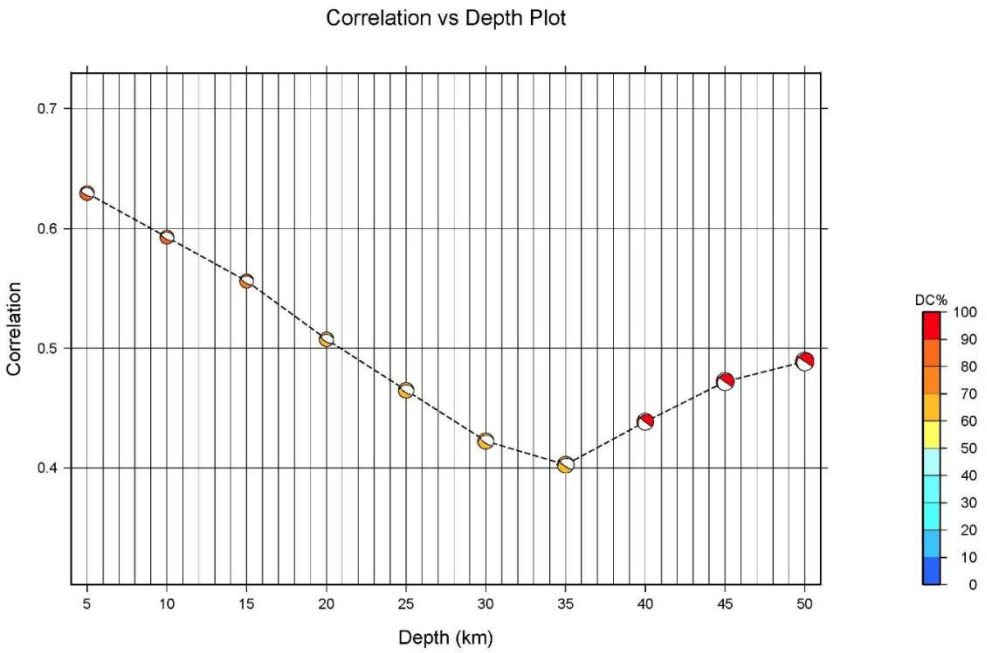

Figure 4.6: (a) and (b) showing aplot the Real-synthetic match at various recording stations and the source depth correlation for a magnitude (Mw > 4.0) earthquake recorded on date 11.11.2012. Grey waveforms are not used in inversion.

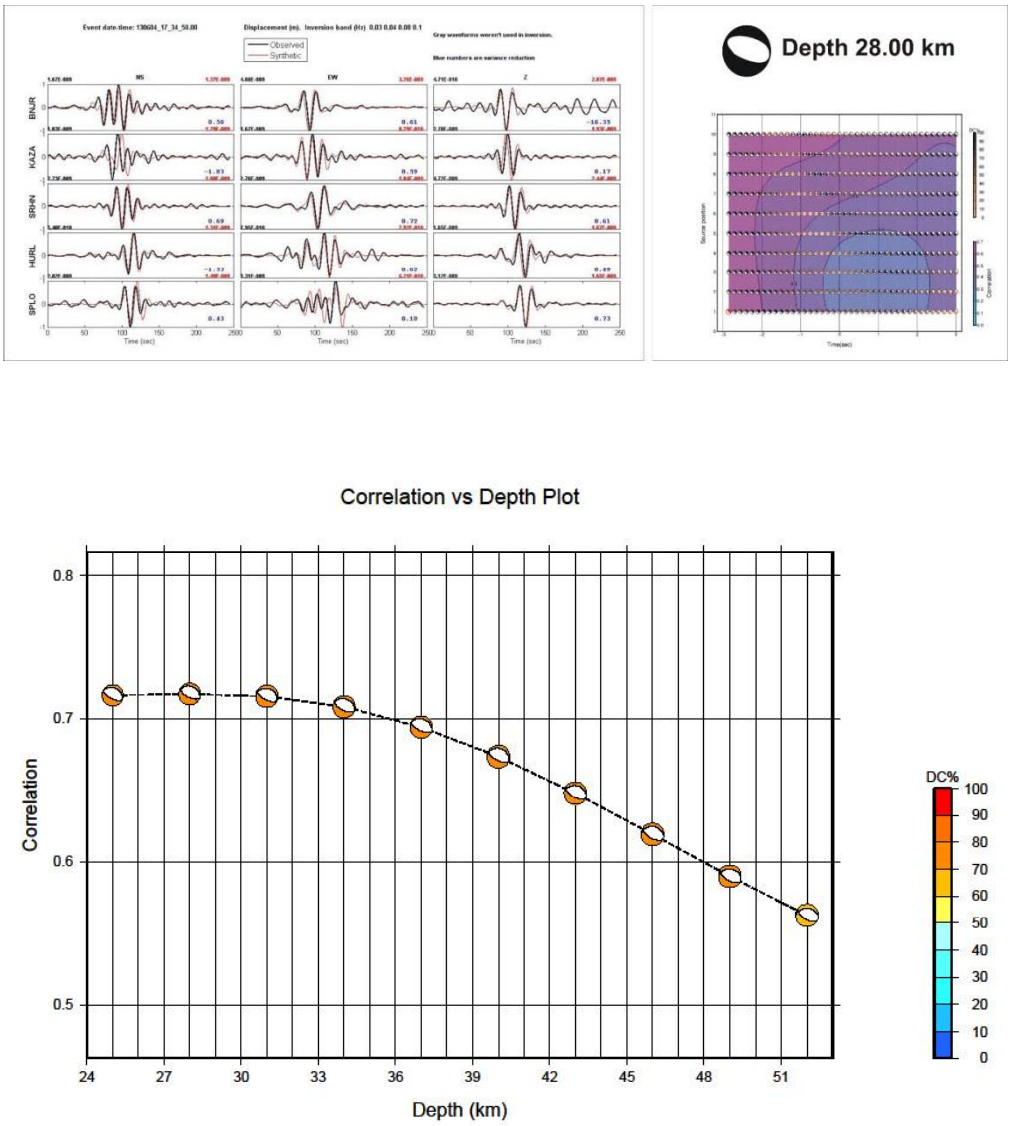

Figure 4.7: (a) and (b) showing aplot the Real-synthetic match at various recording stations and the source depth correlation for a magnitude (Mw > 4.9) earthquake recorded on date 04.06.2013.

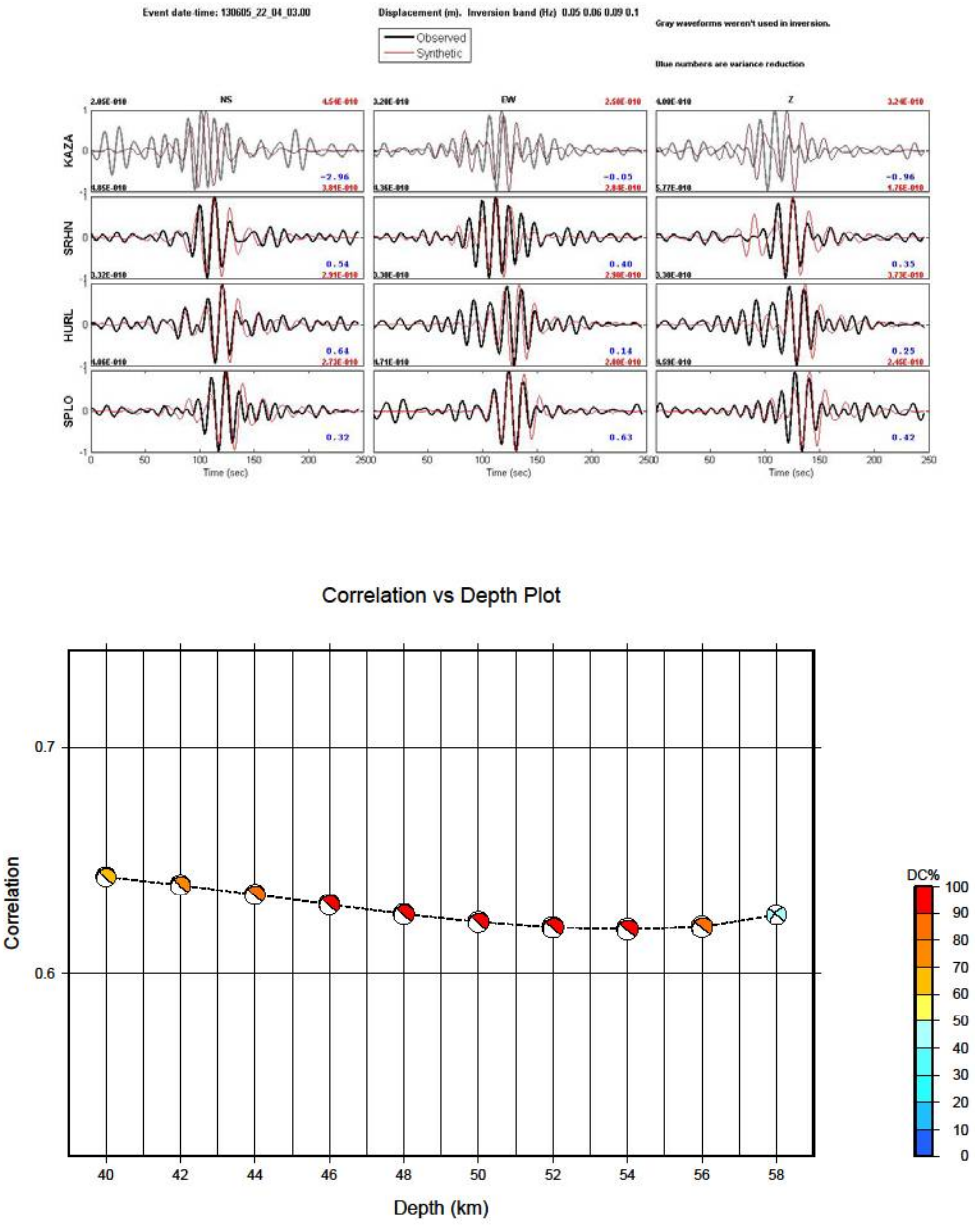

Figure 4.8: (a) and (b) showing aplot the Real-synthetic match at various recording stations and the source depth correlation for a magnitude (Mw > 4.0) earthquake recorded on date 05.06.2013. Grey waveforms are not used in inversion.

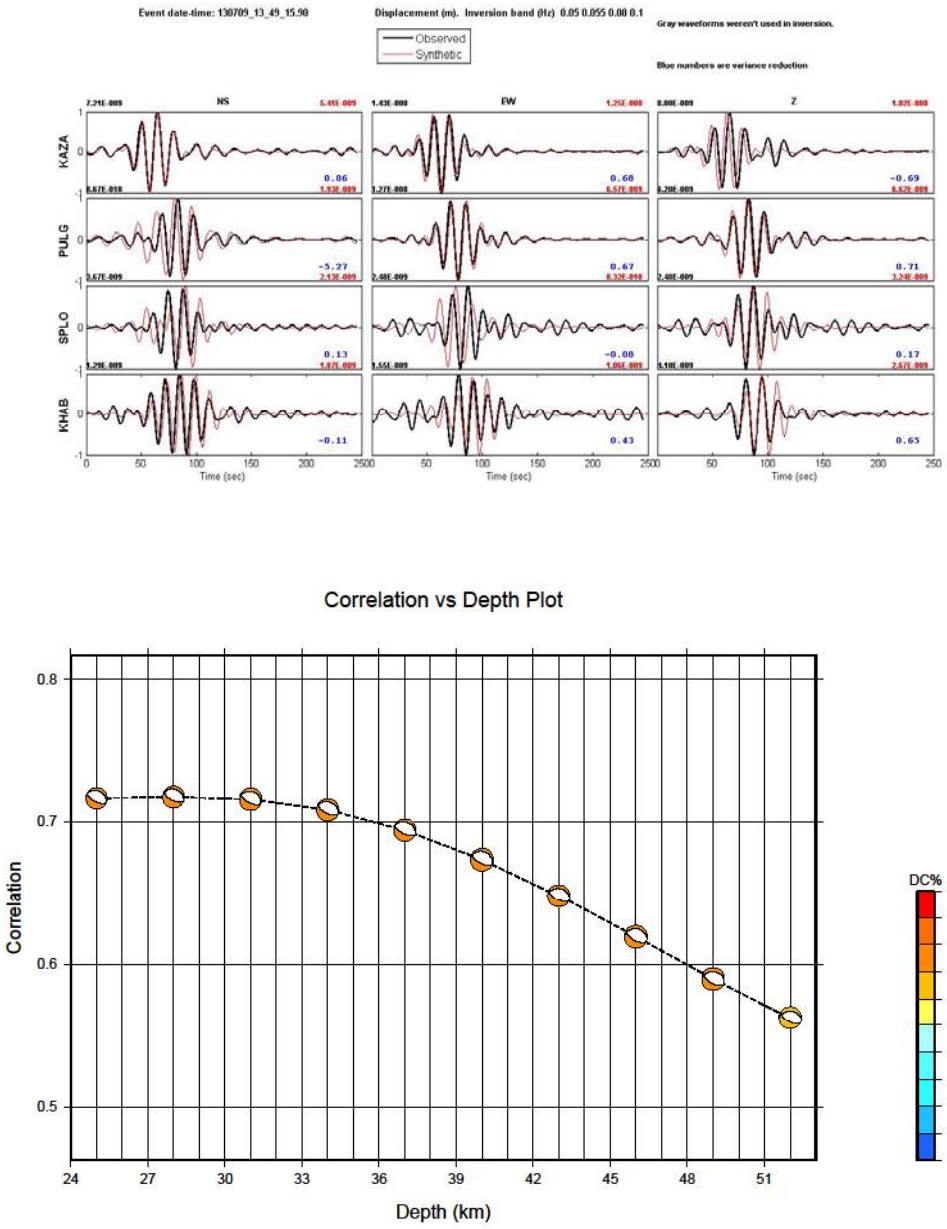

Figure 4.9: (a) and (b) showing aplot the Real-synthetic match at various recording stations and the source depth correlation for a magnitude (Mw > 4.9) earthquake recorded on date 09.07.2013.

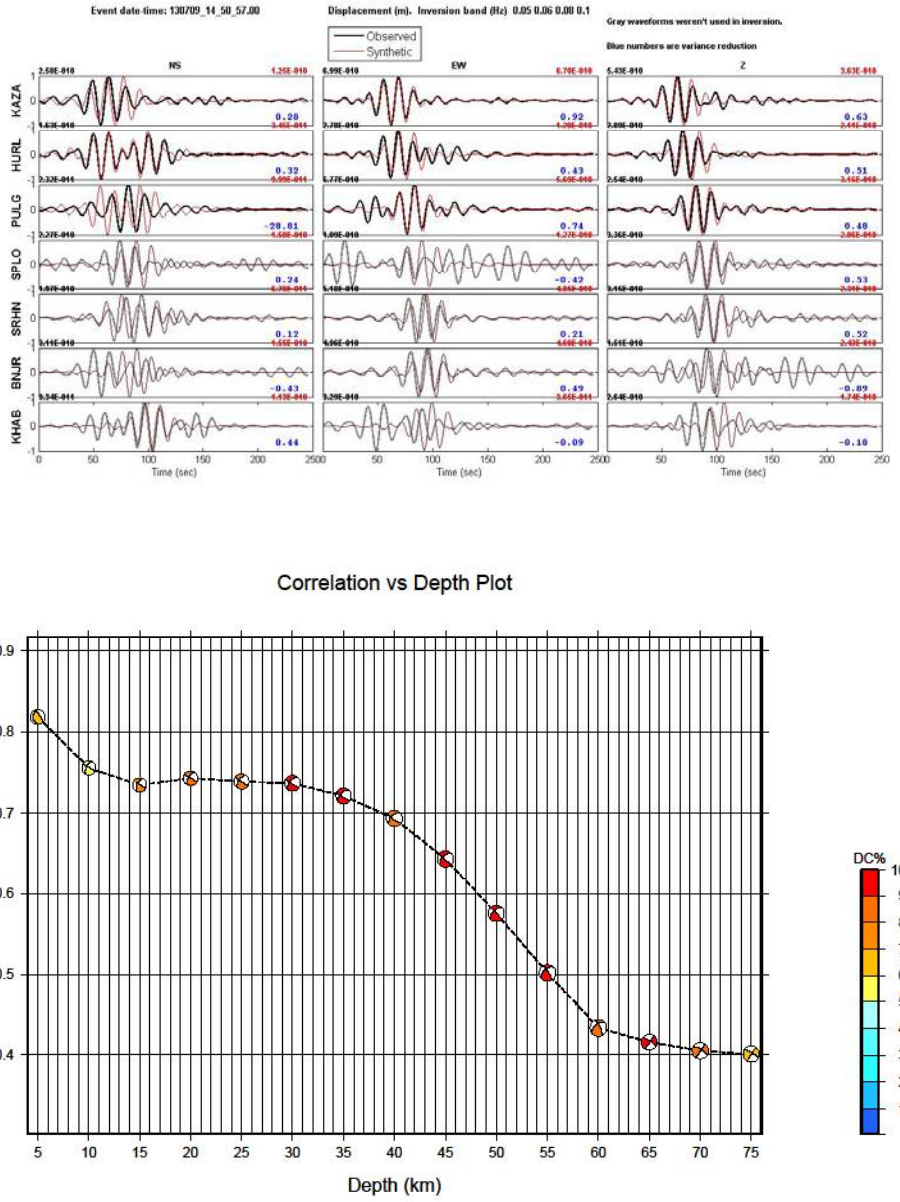

Figure 4.10: (a) and (b) showing aplot the Real-synthetic match at various recording stations and the source depth correlation for a magnitude (Mw > 4.1) earthquake recorded on date 09.07.2013. Grey waveforms are not used in inversion.

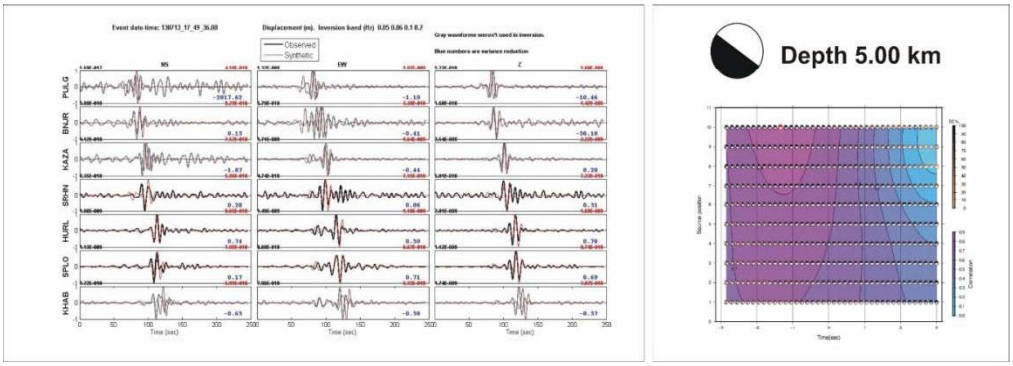

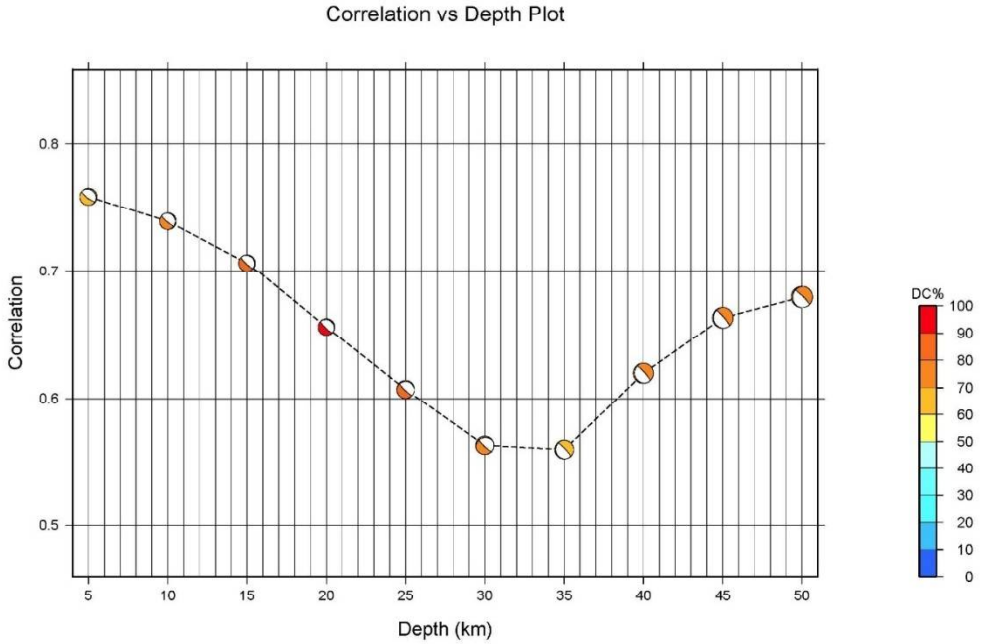

Figure 4.11: (a) and (b) showing aplot the Real-synthetic match at various recording stations and the source depth correlation for a magnitude (Mw > 4.4) earthquake recorded on date 13.07.2013. Grey waveforms are not used in inversion.

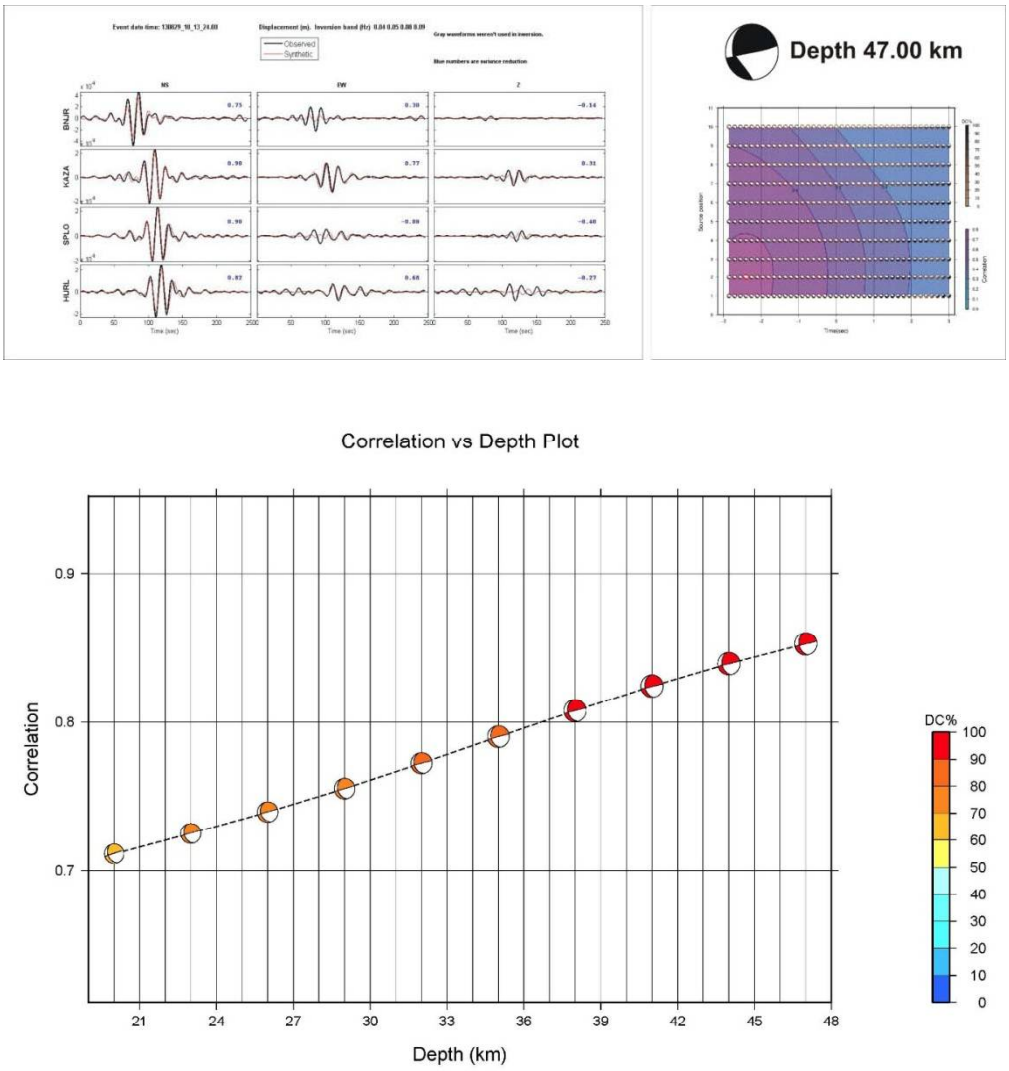

Figure 4.12: (a) and (b) showing aplot the Real-synthetic match at various recording stations and the source depth correlation for a magnitude (Mw > 4.4) earthquake recorded on date 29.08.2013.

4.7. Seismotectonics of the NW Himalaya

Tectonic scenario of the northwest segment of the Himalayan arc is re-examined using the locally and globally recorded earthquake catalogues. For the analysis a maximum of 423 hypoDD relocated events are utilized. The catalogues utilized here include the newly acquired WIHG seismic catalogue and the pre-existing ISC-EHB catalogue over a time period from 2004 to 2013 and 1964 to 2007 in the region. The ISC-EHB catalogue along with the WIHG catalogue events are used for sketching the cross-section across the major tectonic units of the study area as a function of depth. The earthquakes

magnitude ranges from a minimum of 1.8 to 5.6 (M_L) up to a maximum of 50 km depth. The MHT over which Himalaya is placed is continuously deforming in the southward direction through different splay viz. MCT, MBT and HFT with its northward movement. The geometry of the MHT plain varies along the strike of the Himalaya in flat and ramp segments and its dip varies from 4° to 19° below the HFT in south to STD in the north. The depth of the mid crustal ramp and great Himalayan ramp below the MCT (31°N, 77.5°E)and STD (32.2°N, 78.4°E) varies from 12 to 22 km and 28 to 40 km depth respectively. The earthquakes associated with these above tectonic subdivisions are having a focus distribution depth of 2 to 47 km which infers the upper as well as lower crust deformation. The earthquake focus exhibits a bimodal depth distribution characterizing the seismogenic nature of the entire Indian crust. The earthquake associated with the major tectonic breaks shows a wide variation in focal mechanism solutions. The moment tensor solutions obtained (*Table 4.3*) for the study regions inferring a complex tectonic setting are shown in *Figure 4.5 to 4.12*. The brittle –ductile transition zone is inferred at a depth range from 15–20 km in the study area. The above explained seismotectonic setting depicts the multifaceted nature of the NW Himalaya tectonic regime. *Figure 4.13* figure designates the type of kinematics associated with the regional and local tectonic breaks for the study area.A detailed analysis with the incorporation of more modelling techniques like gravity modelling, receiver function inversions may help in understanding the geodynamics of the NW Himalaya.

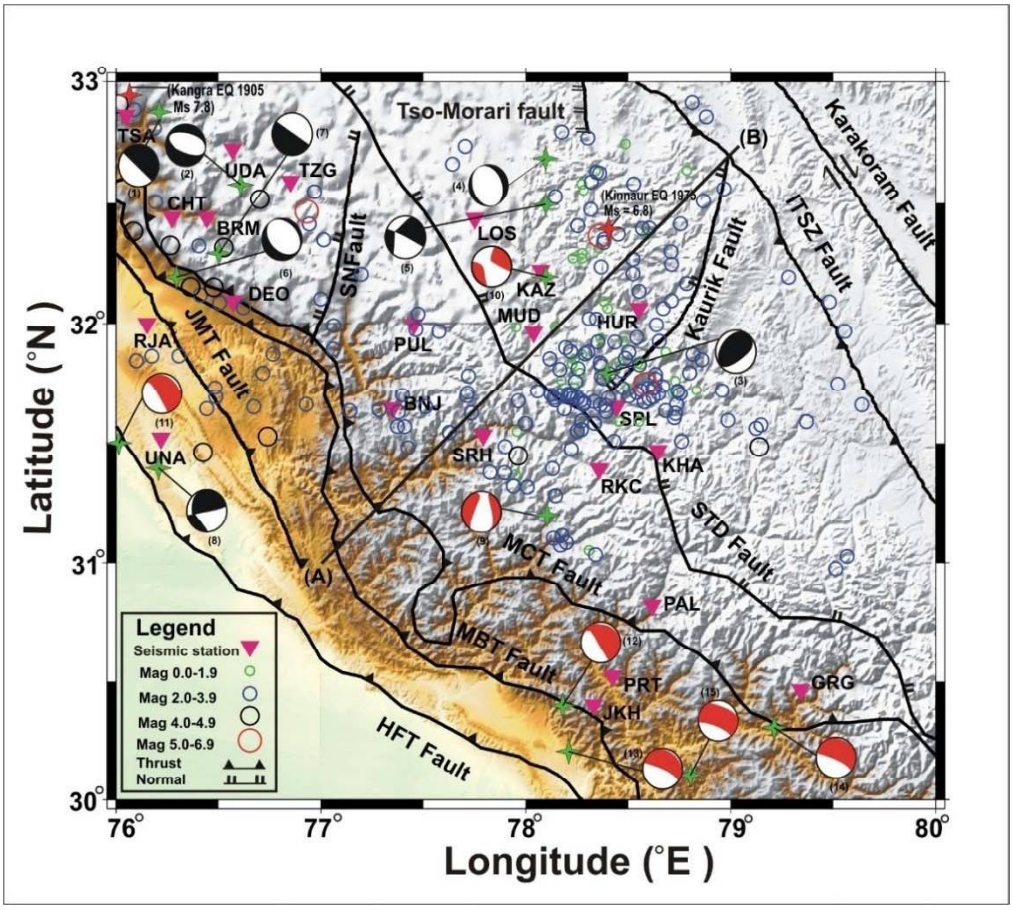

Figure 4.13: This figure designates the type of kinematics associated with the regional and local tectonic breaks for the study area. The black beach balls are the eight moment tensors estimated in this study and the red beach balls are the moment tensors adopted from USGS CMT solutions for the historical earthquakes for the NW Himalaya region. The NE-SW transect AB is also marked in the figure. The earthquake epicentres are designated as hollow blue circles and the eight magnitude (Mw ≥4.0) earthquakes recorded analysed in the present study are shown as green solid stars.

Sl.No. (Ref. Fig 4.13)	Event date	Origin Time	Lat. (°N)	Long (°E)	Depth (km)	Mag. (Mw)	Strike	Dip	Rake	Strike	Dip	Rake	DC %	CLVD %	Source
10	27.02.1983	20:33:06	32.61	78.55	33	5.3	192	71	-7	284	83	-160	-----	----	USGS
11	26.04.1986	07:35:16	32.09	76.31	33	5.5	299	19	58	153	74	100	-----	----	USGS
12	16.07.1986	22:03:10	30.94	77.88	33	5.6	278	17	37	152	80	104	-----	----	USGS
13	19.10.1991	21:23:14	30.74	78.79	19	6.5	317	14	115	112	87	84	-----	----	USGS
14	28.03.1999	19:05:11	30.51	79.4	15	6.4	280	7	75	115	83	92	-----	----	USGS
15	14.12.2005	09:54.2	30.48	79.25	44	5.3	293	23	86	117	64	92	-----	-----	USGS
03	08.10.2012	17:46:20	31.832	78.444	7	4.9	219	38	82	49	52	96	88.1	11.9	Present study
06	11.11.2012	20:23:12	32.294	76.331	5	4	280	24	-105	117	67	-83	87.8	12.2	Present study
01	04.06.2013	17:34:50	32.672	76.601	28	4.9	294	27	-92	117	63	-89	73.7	26.2	Present study
02	05.06.2013	22:04:03	32.907	76.286	47	4	250	16	26	78	89	132	95.5	4.5	Present study
05	09.07.2013	13:49:18	32.765	78.197	8	5	207	54	2	116	89	144	78.9	21.1	Present study
04	09.07.2013	14:50:57	32.743	78.17	5	4.1	324	58	72	176	36	117	62.4	37.6	Present study
07	13.07.2013	17:49:36	32.383	76.535	5	4.4	323	15	15	128	75	-94	60.3	39.7	Present study
08	29.08.2013	10:13:24	31.479	76.273	47	4.4	78	89	89	78	89	132	95.5	4.5	Present study

Table 4.3: A complete set of Focal mechanism parameters determined for earthquakes in the area having a magnitude (M_w) ≥ 4.0 is given below